

Robust Vision-based Nonlinear Formation Control

Omar A.A. Orqueda and Rafael Fierro

Abstract—This paper presents vision-based strategies for decentralized stabilization of *unmanned vehicle (UV)* formations. The key point of the algorithms is that they only require knowledge of leader-follower relative distances or bearing angles. These data are computed using measurements from pan-controlled off-the-shelf cameras on-board following robots, eliminating sensitivity to information flow among vehicles. The approaches are based on output feedback algorithms that use high-gain observers to estimate the derivatives of the UV's relative positions. A Lyapunov stability analysis guarantees that the closed-loop system is stable and the formation error can be made arbitrarily small. A 3D virtual environment and a vision system are used to validate the proposed methodologies.

I. INTRODUCTION

Multi-robot networks are increasingly being considered as a means of performing complex functions within dynamic environments, including such applications as homeland security, search and rescue operations, disaster relief operations, multi-targeting/multi-platform battlefield groups, unmanned combat air vehicle systems, intelligent highway/vehicle systems, and wireless surveillance networks. Creating these types of systems with multiple autonomous vehicles/robots working together to achieve a common mission within a changing environment places severe demands on the design of decision-making supervisors, cooperative control schemes and communication strategies.

Many approaches for solving multi-robot coordination problems reduce to a single-agent control problem by assuming global communication availability. However, a coordination mechanism that does not rely on global communication ensures flexibility and mission safety because reference trajectories and mission objectives should not be shared among all agents but to some leaders [1]. Of course, this poses the challenge of designing robust and computationally simple formation controllers to cope with this problem.

In the last few years, several motion coordination algorithms have been proposed. In [2], authors developed an omnidirectional visual servoing and motion segmentation-based formation control algorithm. Vision-based formation controllers are described in [3]. The algorithms are based on input-output linearization and require the estimation of the leader-follower relative angle and the leader's linear and angular velocities. In [4], authors give a sufficient condition for observability using a vision-based centralized controller. The control law is based on input-output feedback linearization, assuming that the robots have omnidirectional cameras and

the leaders can transmit velocity control to each follower and estimate their states with an extended Kalman filter. Chen *et al.*, [1] propose a decentralized control architecture that employs local sensor information. The information used is relative position and velocity between a robot and its leader. A vision-based formation controller based on nearest-neighbor interactions has been recently developed in [5]. It is assumed that robots move with constant speed and achieve flocking after certain time.

In this paper, we present robust output feedback decentralized controllers based on monocular vision. High-gain observers are used to estimate relative position derivatives. The algorithms eliminate the need of inter-vehicle communication, increasing overall system reliability. We also describe our ongoing implementation on virtual and real platforms.

The rest of the paper is organized as follows. In Section II, we review some definitions on formations. The problem statement is given in Section III. Section IV describes and analyzes the proposed decentralized formation algorithms. Section V summarizes the implementation of the vision system. Section VI provides numerical simulations in a realistic 3D environment. Finally, we present our concluding remarks and future work in Section VII.

II. MATHEMATICAL PRELIMINARIES

In this section, basic concepts on formations are summarized. See [6], [7] for a detailed treatment.

A. Mathematical Model

Let us consider a multi-robot system composed of N_a agents modeled as unicycle-type velocity-controlled vehicles¹ with the kinematic model of the k th robot given by

$$\dot{q}_k(t) = \begin{bmatrix} \cos \theta_k(t) & 0 \\ \sin \theta_k(t) & 0 \\ 0 & 1 \end{bmatrix} u_k(t), \quad (1)$$

where $q_k(t) := [x_k(t), y_k(t), \theta_k(t)]^T \in SE(2)$ is the configuration vector, $u_k(t) := [v_k(t), \omega_k(t)]^T \in \mathcal{U}_k \subseteq \mathbb{R}^2$ is the velocity vector, and \mathcal{U}_k is a compact set of admissible inputs.

Let the Euclidean distance $\ell_{ik}(t) \in \mathbb{R}_{\geq 0}$ and the angles $\alpha_{ik}(t), \beta_{ik}(t) \in (-\pi, \pi]$ between robots i and k be defined as

$$\ell_{ik}(t) := \sqrt{(x_i - x_k^c)^2 + (y_i - y_k^c)^2}, \quad (2)$$

$$\alpha_{ik}(t) := \zeta_{ik} - \theta_i, \quad (3)$$

$$\beta_{ik}(t) := \zeta_{ik} - \theta_k, \quad (4)$$

¹Note that other mathematical models (e.g., a holonomic vehicle $\dot{q}_k = u_k$) can be adapted to this framework.

Omar Orqueda and Rafael Fierro are with MARHES Laboratory, School of Electrical & Computer Engineering, Oklahoma State University, Stillwater, OK 74078-5032, USA. E-mail: orqueda@ieee.org, rfierro@okstate.edu

where $\zeta_{ik}(t) := \text{atan2}(y_i - y_k^c, x_i - x_k^c)$, $x_k^c(t) := x_k + d \cos \theta_k$ and $y_k^c(t) := y_k + d \sin \theta_k$ are the coordinates of the camera, as shown in Figure 1.

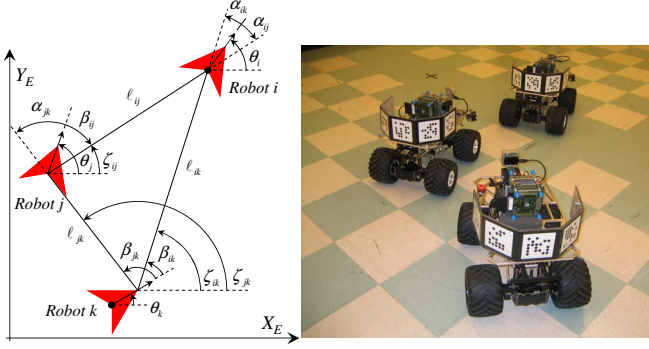


Fig. 1. Formation geometry.

B. Formations

Definition 1 (Formation): A formation is a network of vehicles interconnected via their controller specifications that dictate the relationship each agent must maintain with respect to its leader or leaders. The interconnections between agents are modeled as edges in an acyclic directed graph, labeled by a relationship [7].

Definition 2 (Formation Control Graph): A formation control graph $\mathcal{G} = (\mathcal{V}, \mathcal{E}, \mathcal{S})$ is a directed acyclic graph consisting of the following:

- A finite set $\mathcal{V} = (v_1, \dots, v_{N_a})$ of N_a vertices and a map assigning to each vertex v_k a control system (1).
- An edge set $\mathcal{E} \subset \mathcal{V} \times \mathcal{V}$ encoding leader-follower relationships between agents. The ordered pair $(v_i, v_k) := e_{ik}$ belongs to \mathcal{E} if u_k depends on the state of agent i , q_i .
- A collection $\mathcal{S} = \{s_k\}$ of node specifications defining control objectives, or *set points*, for each node $k : (v_i, v_k), (v_j, v_k) \in \mathcal{E}$ and for some $v_i, v_j \in \mathcal{V}$.

III. PROBLEM STATEMENT

A. Leader-follower algorithm

The first coordination algorithm presented in this paper is based on the relative distance and bearing angle between a robot k and its leader i . Let $s_k(t) \in \mathbb{R}^2$, the node specification of robot k , be given by

$$s_k(t) := [\ell_{ik}(t), \alpha_{ik}(t)]^T. \quad (5)$$

Taking time derivative of (5) we obtain

$$\dot{s}_k(t) = -\varphi(s_k) u_k(t) - \varphi_u(s_k) u_i(t), \quad (6)$$

where $u_k(t) = [v_k(t), \omega_k(t)]^T$, $u_i(t) = [v_i(t), \omega_i(t)]^T$, and

$$\varphi(s_k) := \begin{bmatrix} \cos \beta_{ik} & d \sin \beta_{ik} \\ -\frac{\sin \beta_{ik}}{\ell_{ik}} & \frac{d \cos \beta_{ik}}{\ell_{ik}} \end{bmatrix}, \quad \varphi_u(s_k) := \begin{bmatrix} -\cos \alpha_{ik} & 0 \\ \frac{\sin \alpha_{ik}}{\ell_{ik}} & 1 \end{bmatrix}. \quad (7)$$

Taking the time derivative of (6), we have

$$\begin{aligned} \ddot{s}_k(t) = & -\varphi(s_k) \dot{u}_k(t) - g_0(s_k, u_k) \\ & - g_s(s_k, u_k) \dot{s}_k(t) - g_v(s_k, u_k) V_k(t), \end{aligned} \quad (8)$$

where $V_k(t) = [u_i^T, \dot{u}_i^T, v_i^2, v_j^2, v_i \omega_i, v_j \omega_j, v_i v_j]^T \in \mathbb{R}^6$, and the expressions of $g_0(s_k, u_k) \in \mathbb{R}^2$, $g_s(s_k, u_k) \in \mathbb{R}^{2 \times 2}$, and $g_v(s_k, u_k) \in \mathbb{R}^{2 \times 6}$ are omitted for brevity.

The input matrix transformation $\varphi(s_k)$ in (7) is defined if $\ell_{ik}(t) \geq \ell_{\min} > 0$, where ℓ_{\min} is the minimum distance required to avoid inter-robot collision.

The objective is to design a control law $u_k(t)$, based on $\dot{u}_k(t)$, that allows follower k to track its leader i with a desired specification $s_k^d(t) \in \mathbb{R}^2$, assuming that the leader robot i is stably tracking some desired trajectories $u_i^d(t) := [v_i^d(t), \omega_i^d(t)]^T \in \mathbb{R}^2$ such that $u_i^d(t), \dot{u}_i^d(t), \ddot{u}_i^d(t) \in \mathcal{L}_\infty$.

Let the *specification error* be defined as

$$e_k(t) := s_k^d(t) - s_k(t), \quad e_k(t) \in \mathbb{R}^2. \quad (9)$$

Taking first and second time derivatives of (9) we obtain

$$\dot{e}_k(t) = \varphi(s_k) u_k(t) + \dot{s}_k^d(t) + \varphi_u(s_k) u_i(t), \quad (10)$$

$$\ddot{e}_k(t) = \varphi(s_k) \dot{u}_k(t) + \phi(\dot{s}_k, s_k, u_k) + g_v(s_k, u_k) V_k(t), \quad (11)$$

with

$$\phi(\dot{s}_k, s_k, u_k) := \dot{s}_k^d + g_0(s_k, u_k) + g_s(s_k, u_k) \dot{s}_k(t). \quad (12)$$

B. Two-leader algorithm

The second coordination algorithm presented in this paper is based on the relative distances between the follower robot k and its leaders i and j . Let $s_k(t) \in \mathbb{R}^2$, the specification of robot k , be given by

$$s_k(t) := [\ell_{ik}(t), \ell_{jk}(t)]^T. \quad (13)$$

Taking the time derivative of (13), we obtain

$$\dot{s}_k(t) = -\varphi(s_k) u_k(t) - \varphi_u(s_k) U_{ij}(t), \quad (14)$$

where

$$\varphi(s_k) := \begin{bmatrix} \cos \beta_{ik} & d \sin \beta_{ik} \\ \cos \beta_{jk} & d \sin \beta_{jk} \end{bmatrix}, \quad (15)$$

$$\varphi_u(s_k) := \begin{bmatrix} -\cos \alpha_{ik} & 0 \\ 0 & -\cos \alpha_{jk} \end{bmatrix}, \quad (16)$$

with $\alpha_{jk} = \zeta_{jk} - \theta_j$, $\beta_{jk} = \zeta_{jk} - \theta_k$, as shown in Figure 1, and $U_{ij}(t) := [v_i(t), v_j(t)]^T$. Let us define $\vec{\tau}_\alpha := [c_\alpha, s_\alpha]^T$, using the time derivative of the triangle equality

$$\ell_{ik} \vec{\tau}_{\zeta_{ik}} = \ell_{ij} \vec{\tau}_{\zeta_{ij}} + \ell_{jk} \vec{\tau}_{\zeta_{jk}},$$

and taking the second time derivative of (13), we obtain

$$\begin{aligned} \ddot{s}_k(t) = & -\varphi(s_k) \dot{u}_k(t) - g_0(s_k, u_k) \\ & - g_s(s_k, u_k) \dot{s}_k(t) - g_v(s_k, u_k) V_k(t), \end{aligned} \quad (17)$$

where $V_k(t) := [U_{ij}^T, \dot{U}_{ij}^T, v_i^2, v_j^2, v_i \omega_i, v_j \omega_j, v_i v_j]^T \in \mathbb{R}^9$, and the expressions for $g_0(s_k, u_k) \in \mathbb{R}^2$, $g_s(s_k, u_k) \in \mathbb{R}^{2 \times 2}$, and $g_v(s_k, u_k) \in \mathbb{R}^{2 \times 6}$ are omitted for brevity.

Note that $\dot{s}_k(t)$ and $\varphi^{-1}(s_k)$ are not defined when $\zeta_{ij} := \zeta_{ik} - \zeta_{jk} = 0$, *i.e.*, when one of the robots obstructs the line of sight of the other one or when both robots occupy the same point. The former case must be avoided due to the lack of sensor data by switching to a leader-follower controller, whereas the latter is impossible due to collision.

The objective is to design a control law $u_k(t)$, based on $\dot{u}_k(t)$, such that robot k can track its leader robots i and j . Assuming that leader robot i is stably tracking some desired trajectory $u_i^d(t) := [v_i^d(t), \omega_i^d(t)]^T \in \mathbb{R}^2$ and leader robot j maintains a formation specification with respect to robot i . Moreover, the trajectory of leader robot j verifies $u_j(t)$, $\dot{u}_j(t)$, $\ddot{u}_j(t) \in \mathcal{L}_\infty$, due to the stability properties of a leader-follower algorithm.

Let the *specification error* be defined as in (10)

$$e_k(t) := s_k^d(t) - s_k(t), \quad e_k(t) \in \mathbb{R}^2. \quad (18)$$

By taking first and second time derivatives of (18), we obtain similar expressions as in (10) and (11). Then, stability properties of both algorithms can be analyzed in similar fashion by using these error dynamics.

Let the filtered error signal $r_k(t) \in \mathbb{R}^2$ be defined as

$$r_k(t) := \dot{e}_k(t) + K e_k(t) \quad (19)$$

with $K = \text{diag}(k_1, k_2)$, k_1 and $k_2 \in \mathbb{R}^+$ gain constants. Differentiating (19) with respect to time and using (11) yields

$$\begin{aligned} \dot{r}_k(t) &= \varphi(s_k) \dot{u}_k(t) + \phi(\dot{s}_k, s_k, u_k) \\ &\quad + g_v(s_k, u_k) V_k(t) + K \dot{e}_k(t). \end{aligned} \quad (20)$$

IV. OUTPUT FEEDBACK (OFB) ALGORITHM

The design of a controller for (20) can be made using three levels of information: The first level, and the most complex from the point of view of information flow, is given by the knowledge of the velocities and accelerations of the leaders, the specification, and its derivative. The second level requires the knowledge of the specification and its derivative. Finally, the third only requires the knowledge of the specification.

In this paper, we propose *output feedback* (OFB) algorithms which only use the simplest information level, *i.e.*, the knowledge of the edge specification $s_k(t)$.

Let the unknown state $\dot{s}_k(t)$ be *estimated* using a *high-gain observer* (HGO) following the lines of [8] as follows

$$\dot{\hat{s}}_1(t) = \hat{s}_2(t) + \frac{\alpha_1}{\varepsilon} (s_k(t) - \hat{s}_1(t)) \quad (21)$$

$$\begin{aligned} \dot{\hat{s}}_2(t) &= -\varphi(s_k, u_k) \dot{u}_k(t) - g_s(s_k, u_k) \hat{s}_2 \\ &\quad + \frac{\alpha_2}{\varepsilon^2} (s_k(t) - \hat{s}_1(t)), \end{aligned} \quad (22)$$

where $\alpha_1, \alpha_2 \in \mathbb{R}_{>0}^{2 \times 2}$, the HGO gains, are constant diagonal matrices, and $\varepsilon \in \mathbb{R}_{>0}$, the HGO constant, is designed such that the estimated values $\hat{s}_1(t)$ and $\hat{s}_2(t)$ converge to the real values $s_k(t)$ and $\dot{s}_k(t)$, respectively, fast enough to stabilize the whole system.

Let the estimation error vector $\eta(t)$ be defined as $\eta(t) := [\eta_1^T(t), \eta_2^T(t)]^T \in \mathbb{R}^4$, with

$$\eta_1(t) = \frac{1}{\varepsilon} (s_k(t) - \hat{s}_1(t)), \quad (23)$$

$$\eta_2(t) = \dot{s}_k(t) - \hat{s}_2(t). \quad (24)$$

Using (21) to (24), the observer error dynamics become

$$\varepsilon \dot{\eta}(t) = A_0 \eta(t) + \varepsilon f(t), \quad (25)$$

where $A_0 = \begin{bmatrix} -\alpha_1 & I_2 \\ -\alpha_2 & 0_2 \end{bmatrix} \in \mathbb{R}^{4 \times 4}$, $0_2 \in \mathbb{R}^{2 \times 2}$ is a null matrix, $I_2 \in \mathbb{R}^{2 \times 2}$ is an identity matrix, and

$$f(t) = \begin{bmatrix} 0 \\ -g_s(s_k, u_k) \eta_2 - g_v(s_k, u_k) V_k(t) \end{bmatrix} \in \mathbb{R}^4.$$

If $\varepsilon \rightarrow 0$ and $d\tau = \frac{1}{\varepsilon} dt$ in equation (25), then

$$\frac{d\eta(\tau)}{d\tau} = A_0 \eta(\tau). \quad (26)$$

Equation (26) is called the *boundary layer system*.

Let the OFB controller be defined as

$$\begin{aligned} \dot{u}_k(t) &= -\varphi^{-1}(s_k, u_k) \left[\phi(\hat{s}_2, s_k, u_k) + 2K \left(\dot{s}_k^d(t) - \hat{s}_2(t) \right) \right. \\ &\quad \left. + K^2 e_k(t) + \bar{u}_k(t) \right] \end{aligned} \quad (27)$$

where $\bar{u}_k(t) \in \mathbb{R}^2$ is an auxiliary control law given by

$$\bar{u}_k(t) := \beta(t) \text{sign}(e_k(t)), \quad (28)$$

where $\beta(t) \in \mathbb{R}_{>0}$ is a positive control gain.

The closed-loop formation specification error dynamic model under the OFB algorithm (27) is

$$\begin{aligned} \dot{r}_k(t) &= -K r_k(t) - 2K \eta_2(t) + g_s(s_k, u_k) \eta_2(t) \\ &\quad + g_v(\dot{s}_k, s_k, u_k) V_k(t) - \bar{u}_k(t). \end{aligned} \quad (29)$$

Theoretically, the observer error will not cause the system to become unstable using the OFB controller (27), but it is necessary to use saturation to prevent over-exceeding the control strength when the observer error is too large.

Before presenting the main result of this paper, Theorem 1, it is necessary to state the following lemma:

Lemma 1: Let the auxiliary function $L(t) \in \mathbb{R}$ be defined as

$$L(t) := r_k^T(t) [g_v(t) V_k(t) - \bar{u}_k(t)]. \quad (30)$$

with $g_v(t) = g_v(s_k(t), u_k(t))$. If the control gain β is selected to satisfy the sufficient condition

$$\beta > \|g_v(t) V_k(t)\|_2 + \underline{k}_{12}^{-1} \left\| \frac{d[g_v(t) V_k(t)]}{dt} \right\|_2,$$

where K is given in (19) and $\underline{k}_{12} := \min(k_1, k_2)$. Then

$$\int_{t_0}^t L(\tau) d\tau < \zeta_b,$$

where the positive constant $\zeta_b \in \mathbb{R}^+$ is defined as

$$\zeta_b := \beta \|e_k(t_0)\|_1 - e_k^T(t_0) [g_v(t_0) V_k(t_0)], \quad (31)$$

and $\|\cdot\|_1$ denotes the \mathcal{L}_1 norm.

Proof: The proof of this Lemma is given in [9]. ■

Theorem 1: The control law (27) with the observer (21)-(22) ensure that the combined closed-loop system (25) and (29) exponentially converge to an arbitrarily small neighborhood about the origin of the specification error.

Proof: The proof follows the guidelines of [10]. It is done in three steps: The first step proves that there exists an invariant set for the closed-loop output feedback system based on a composite Lyapunov function. The second step shows that any trajectory will be trapped into this invariant

set in finite time if the HGO constant ε is chosen small enough. The third step demonstrates that this invariant set is globally uniformly ultimately bounded (GUUB).

First step - Let $W_1(t)$ be a non-negative functions defined as

$$W_1(t) := \frac{1}{2} r_k^T(t) r_k(t) + P(t), \quad (32)$$

where $P(t) := \zeta_b - \int_{t_0}^t L(\tau) d\tau$, $P(t) \in \mathbb{R}_{>0}$ is an auxiliary function.

Let $\mathcal{R} = \mathbb{R}^2$ be the region of attraction of the system (10)-(11) with the control law (27). Let \mathcal{D}_r be a compact set in the interior of \mathcal{R} . Let \mathcal{D}_c be defined by $\mathcal{D}_c := \{r_k(t) \in \mathcal{R} \mid W_1(t) \leq c\}$, where $W_1(t)$ is defined in (32) and $c > \max_{r_k \in \mathcal{D}_r} W_1(t)$ is a positive constant. The set \mathcal{D}_c is a compact subset of \mathcal{R} and \mathcal{D}_r is in the interior of \mathcal{D}_c .

For the boundary layer system, let $W_2(\eta)$ be defined as

$$W_2(\eta) := \eta^T P_0 \eta, \quad (33)$$

where $P_0 \in \mathbb{R}^{4 \times 4}$ is a positive definite matrix such that $P_0 A_0 + A_0^T P_0 = -I_4$, with A_0 defined in (26). Let the compact set \mathcal{D}_ε be defined by $\mathcal{D}_\varepsilon := \{\eta(t) \in \mathbb{R}^4 \mid W_2(t) \leq \rho \varepsilon^2\}$, where ρ is a positive constant to be selected later and ε is the HGO constant. Finally, let the set Σ_c be defined by $\Sigma_c := \mathcal{D}_c \times \mathcal{D}_\varepsilon$.

The derivative of (32) for $(e_k(t), \dot{e}_k(t), \eta(t)) \in \{W_1(t) = c\} \times \mathcal{D}_\varepsilon$ verifies

$$\begin{aligned} \dot{W}_1(t) &\leq -k_{12} \left[\|r_k(t)\|^2 - \sigma_1 \|\eta(t)\| \right] \\ &\leq -k_{12} (\mu - L_1 \varepsilon), \end{aligned} \quad (34)$$

with $\sigma_1 := \frac{\sigma_s + 2\bar{k}_{12}}{\bar{k}_{12}}$, $\sigma_s := \max_{s_k, u_k} \|g_s(s_k, u_k)\|$, $\bar{k}_{12} := \lambda_{\max}(K)$, $\mu = \min_{r_k \in \partial \mathcal{D}_c} \{\|r_k(t)\|^2\}$, and $L_1 := \sigma_1 \sqrt{\frac{\rho}{\lambda_{\min}(P_0)}}$.

Analyzing the derivative of (33) for $(e_k(t), \dot{e}_k(t), \eta(t)) \in \mathcal{D}_c \times \{W_2(t) = \rho \varepsilon^2\}$ we find

$$\begin{aligned} \dot{W}_2(t) &\leq -\frac{\|\eta(t)\|^2}{2\varepsilon} [1 - 4\|P_0\| \sigma_s \varepsilon] \\ &\quad - \frac{\|\eta(t)\|}{2\varepsilon} [\|\eta(t)\| - 4\|P_0\| \sigma_v \varepsilon] \\ &\leq -\frac{\|\eta(t)\|^2}{2\varepsilon} (1 - 4\|P_0\| \sigma_s \varepsilon) \\ &\quad - \frac{\|\eta(t)\|}{2} \left(\sqrt{\frac{\rho}{\|P_0\|}} - 4\|P_0\| \sigma_v \right), \end{aligned} \quad (35)$$

with $\sigma_v := \max_{s_k, u_k, u_i, u_j} \|g_v(s_k, u_k) V_k(t)\|$, and $\|P_0\| := \lambda_{\max}(P_0)$.

Taking $\rho = 16\sigma_v^2 \lambda_{\max}^3(P_0)$ and $\varepsilon_1 = \min\left(\frac{1}{4\sigma_s \|P_0\|}, \frac{\mu}{L_1}\right)$, for every $0 < \varepsilon \leq \varepsilon_1$, we have

$$\dot{W}_1(t) \leq 0,$$

for $(e_k(t), \dot{e}_k(t), \eta(t)) \in \{W_1(t) = c\} \times \mathcal{D}_\varepsilon$, and

$$\dot{W}_2(t) \leq 0,$$

for $(e_k(t), \dot{e}_k(t), \eta(t)) \in \mathcal{D}_c \times \{W_2(t) = \rho \varepsilon^2\}$. Therefore, $\Sigma_c := \mathcal{D}_c \times \mathcal{D}_\varepsilon$ is a positively invariant set.

Second step - Let the initial state satisfy $(e_k(0), \dot{e}_k(0), \eta(0)) \in \mathcal{D}_r \times \mathcal{Q}$, where \mathcal{Q} is a compact set such that $\mathcal{Q} \subseteq \mathbb{R}^4$. Using (23)-(24) it can be seen that

$$\|\eta(0)\| \leq \frac{c_3}{\varepsilon},$$

where $c_3 \in \mathbb{R}_{>0}$ is an appropriate constant. Because $(e_k(0), \dot{e}_k(0)) \in \mathcal{D}_r$, we have

$$\begin{aligned} \|e_k(t) - e_k(0)\| &\leq c_2^a t, \\ \|\dot{e}_k(t) - \dot{e}_k(0)\| &\leq c_2^b t, \\ \|r_k(t) - r_k(0)\| &\leq c_2 t, \end{aligned} \quad (36)$$

where $c_2^b, c_2^a, c_2 \in \mathbb{R}_{>0}$ are some positive constants. Therefore, there exists a finite time T_0 , independent of ε , such that $(e_k(t), \dot{e}_k(t)) \in \mathcal{D}_r$ for all $t \in [0, T_0]$. In consequence, if $t \in [0, T_0]$ and $W_2(\eta(t)) \geq \rho \varepsilon^2$, $\dot{W}_2(t) \leq -\frac{1}{2\varepsilon} \|\eta(t)\|^2$ from (35). Then

$$\dot{W}_2(t) \leq -\frac{\mu_1}{\varepsilon} W_2(t), \quad (37)$$

with $\mu_1 := \frac{1}{2\|P_0\|}$. The solution for (37) is

$$W_2(t) \leq \frac{\mu_2}{\varepsilon^2} \exp\left(-\frac{\mu_1}{\varepsilon} t\right), \quad (38)$$

with $\mu_2 := c_3^2 \|P_0\|$. As it can be seen from (38), $\lim_{t \rightarrow \infty} W_2(t) = 0$. Let T_ε be the time for which $W_2(t)$ falls below to $\rho \varepsilon^2$, it must satisfy

$$W_2(\eta(T_\varepsilon)) \leq \frac{\mu_2}{\varepsilon^2} \exp\left(-\frac{\mu_1}{\varepsilon} T_\varepsilon\right) \leq \rho \varepsilon^2, \quad (39)$$

In consequence, $T_\varepsilon \geq \frac{\varepsilon}{\mu_1} \ln\left(\frac{\mu_2}{\rho \varepsilon^4}\right)$ and $\lim_{\varepsilon \rightarrow 0} T_\varepsilon = 0$. Then, it is possible to choose ε_2 small enough such that $T_\varepsilon = \frac{1}{2} T_0$, for all $\varepsilon \in (0, \varepsilon_2]$. It follows that $W_2(\eta(T_\varepsilon)) < \rho \varepsilon^2$ for all $\varepsilon \in (0, \varepsilon_2]$. Choosing $\varepsilon_1^* = \min(\varepsilon_1, \varepsilon_2)$, the trajectory $(e_k(t), \dot{e}_k(t), \eta(t))$ enters into the invariant set Σ_c in $t \in [0, T_\varepsilon]$ and remains in Σ_c , for all $t \geq T_\varepsilon$ and every $0 < \varepsilon \leq \varepsilon_1^*$. Moreover, the trajectory $(e_k(t), \dot{e}_k(t), \eta(t))$ is bounded by (36) and (38), for $t \in [0, T_\varepsilon]$ and $\varepsilon \in (0, \varepsilon_1^*]$.

Third step - If the initial state satisfies $(e_k(0), \dot{e}_k(0), \eta(0)) \in \mathcal{D}_r \times \mathcal{Q}$, then the trajectory of the system will be inside Σ_c , for all $t \geq T_\varepsilon$ and $0 < \varepsilon \leq \varepsilon_1^*$. Because, from (38), $\lim_{\varepsilon \rightarrow 0} W_2(\eta(t)) = 0$, it is possible to find $\varepsilon_3 = \varepsilon_3(\delta_0) \leq \varepsilon_1^*$, for any given small value δ_0 , such that

$$\|\eta(t)\| \leq \frac{\delta_0}{2}, \quad (40)$$

for $t \geq T_{\varepsilon_3} = T_{\varepsilon_3}(\delta_0)$.

Let the compact sets \mathcal{D}_1 and \mathcal{D}_2 be given by

$$\mathcal{D}_1 := \{(e_k(t), \dot{e}_k(t)) \in \mathcal{R} : \|r_k(t)\|^2 \leq 2L_1 \varepsilon\}, \quad (41)$$

and

$$\mathcal{D}_2 := \{(e_k(t), \dot{e}_k(t)) \in \mathcal{R} : W_1(t) \leq v(\varepsilon)\}, \quad (42)$$

with $v(\varepsilon) := \max_{\|r\|^2 < 2L_1 \varepsilon} \{W_1(t)\}$. If $(e_k(t), \dot{e}_k(t)) \notin \mathcal{D}_1$,

$$\dot{W}_1(t) \leq -\frac{1}{2} k_{12} \|r_k(t)\|^2.$$

Let $\varepsilon_4 = \varepsilon_4(\delta_0)$ be chosen such that \mathcal{D}_2 is in the interior of \mathcal{D}_c and

$$\mathcal{D}_2 \subset \left\{ (e_k(t), \dot{e}_k(t)) \in \mathcal{R} : \|e_k(t)\| \leq \frac{1}{4}\delta_0, \|\dot{e}_k(t)\| \leq \frac{1}{4}\delta_0 \right\}.$$

Then for all $(e_k(t), \dot{e}_k(t)) \in \mathcal{D}_c$, $(e_k(t), \dot{e}_k(t)) \notin \mathcal{D}_2$,

$$\dot{W}_1(t) \leq -\frac{1}{2}k_{12}\|r_k(t)\|^2.$$

Therefore, the set $\Sigma_1 := \mathcal{D}_2 \times \mathcal{D}_\varepsilon$ is positively invariant and every trajectory in $\mathcal{D}_c \times \mathcal{D}_\varepsilon$ enters Σ_1 in finite time $T_{\varepsilon_4} = T_{\varepsilon_4}(\delta_0)$, for $\varepsilon \in (0, \varepsilon_4]$. Let $\varepsilon_2^* = \min\{\varepsilon_3, \varepsilon_4\}$ and $T_1 = \max\{T_{\varepsilon_3}, T_{\varepsilon_4}\}$, therefore

$$\|e_k(t)\| + \|\dot{e}_k(t)\| + \|\eta(t)\| \leq \delta_0, \quad (43)$$

with $\delta_0 > 0$, $\varepsilon \in (0, \varepsilon_2^*]$, and $t \geq T_1$. Then $(e_k(t), \dot{e}_k(t), \eta(t))$ is GUUB. ■

V. REAL AND ARTIFICIAL VISION SYSTEMS

In this section we briefly describe the vision system used in this work. This system estimates pose from single frames using fiducial markers. Pose estimation using fiducial markers has been addressed by augmented reality applications in order to combine virtual 3D representations with the real world for active interaction [11].

In this work, each robot is equipped with a *PC104* embedded computer, a monochromatic camera (*Unibrain Fire-I* or *Point Grey's Bumblebee*) and a truncated regular octagon shape with five identification tags, as shown in Figure 1.

The identification method consists in two stages as follows: (i) A *training* stage used to create a database with the marker ID number (this ID number is computed by a binary string whose position number is 1 if the square is filled and 0 otherwise, as shown in Figure 2); (ii) An *identification* stage that consists of transforming the center point of each square region to the collineated space to take into account perspective distortion and detect if the square is filled. Then, the fiducial marker is obtained using the on-line recovered ID and the database previously created.

Finally, relative distance and orientation are computed using markers positions with respect to the robot reference frame.

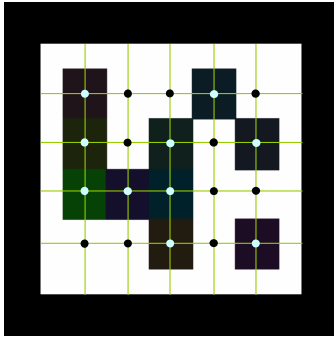


Fig. 2. ID of the fiducial marker.

The vision library is implemented on *MPSLab*, a motion planning, simulation, and virtual perception library capable of accurately simulate systems in 3D environments [12], as shown in Figure 3.

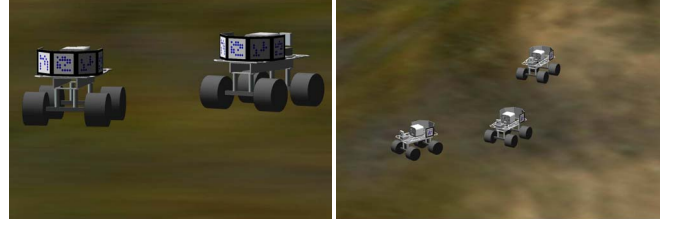


Fig. 3. Virtual camera screenshots from [12].

VI. SIMULATION RESULTS

In this section, some simulations are presented that validate the performance of the decentralized observer/controller pair proposed herein. All simulations were written in C++ on a Linux platform using *MPSLab*.

The initial positions of the robots in the simulations experiments are $q_\ell(0) = [0, -5, 0]^T$, $q_1(0) = [-3, -8, 0]^T$, $q_2(0) = [-3, -2, 0]^T$, $q_3(0) = [-3, -10, 0]^T$, $q_4(0) = [-3, -6, 0]^T$, $q_5(0) = [-3, -4, 0]^T$, $q_6(0) = [-3, 0, 0]^T$, and their initial velocities are equal to 0.0 m/sec. The parameters of the controllers are $k_1 = k_2 = \beta = 5.0$, the sampling time is 10msec, and we used the function

$$\bar{u}_k(t) := \beta \tanh(24.53e(t)),$$

instead of (28) to avoid excessive chattering.

Figures 5-7 show simulations when the leader follows a circular trajectory and the followers have the specifications shown in Figure 4. The decentralized controller is able to drive each robot to the desired specification, given by a relative distance and bearing angle or by two relative distances. Figure 5 shows the trajectories of the robots using both OFB controllers with $\varepsilon = 0.01$. Figure 6 shows the control inputs and the specification error of robot 2 using a leader-follower algorithm. Figure 7 shows the control inputs and the specification error of robot 5 using a two-leader algorithm. Despite of the lack of knowledge about the leader or leaders state, the behavior is quite satisfactory using any of the OFB observer/controller pairs.

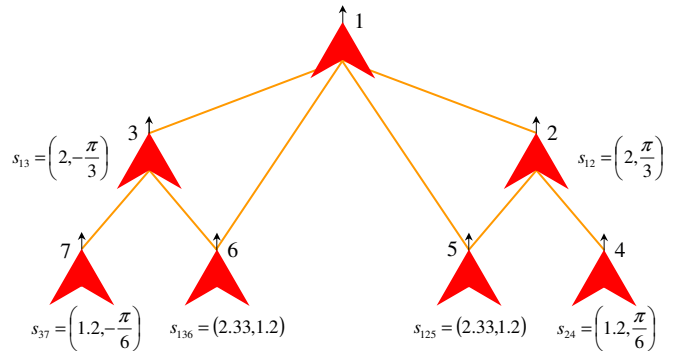


Fig. 4. Specifications for 7 robots.

VII. CONCLUSIONS

In this paper, we present robust vision-based output feedback decentralized observer/controller pairs based only on the relative position between a robot and its designated

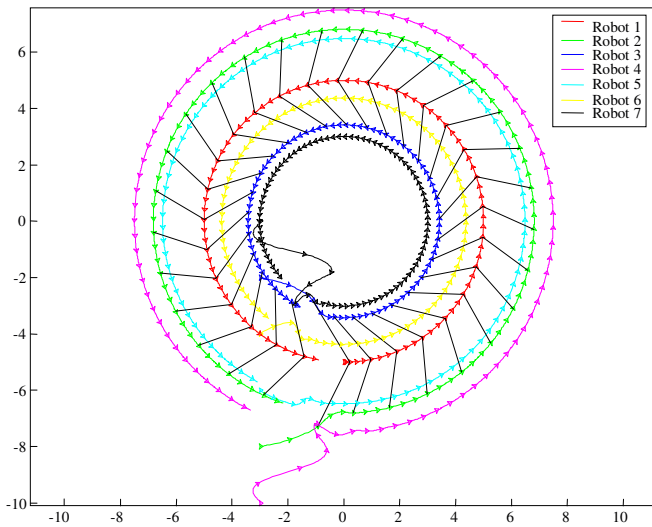


Fig. 5. Trajectories of the robots.

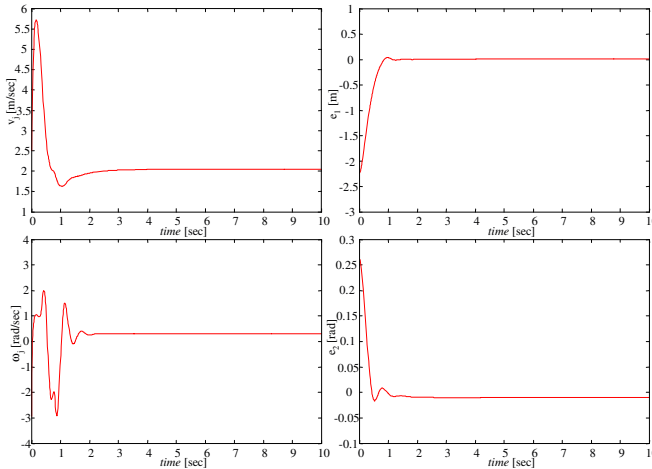


Fig. 6. Velocities and error of robot 2 using the leader-follower algorithm.

leaders. High-gain observers are used to estimate derivatives from visual data. The algorithms eliminate the need of inter-vehicle communication which increases the reliability of the overall system.

The first method requires the relative distance and bearing angle between a robot and a leader. The second approach requires relative distances between a robot and two leaders. The stability properties of both approaches are guaranteed using Lyapunov theory. Simulations in a realistic 3D environment validate the performance of the output feedback observer/controller pairs.

Currently, these multi-vehicle decentralized coordination methodologies are being tested on actual car-like mobile robots. Future research will focus on observability properties of dynamic graphs and on the relationship between observability and connectivity of graphs.

VIII. ACKNOWLEDGMENTS

This work is supported in part by NSF grants #0311460 and CAREER #0348637 and by the U.S. Army Research Office under grant DAAD19-03-1-0142 (through the University

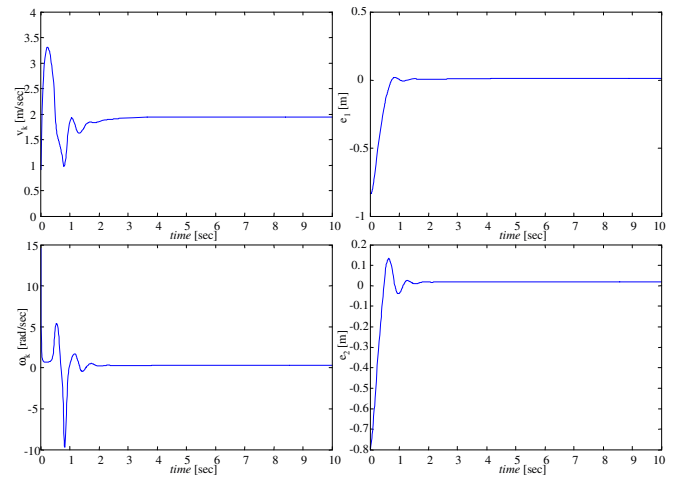


Fig. 7. Velocities and error of robot 5 using the two-leader algorithm.

of Oklahoma.)

The authors would like to thank Dr. Tony Zhang for helpful discussions on the formulation of the OFB controller.

REFERENCES

- [1] X. Chen, A. Serrani, and H. Özbay, "Control of leader-follower formations of terrestrial uavs," in *Proceedings of the 42nd IEEE Conference on Decision and Control*, no. 1, (Maui, Hawaii USA), pp. 498–503, Dec. 2003.
- [2] R. Vidal, O. Shakernia, and S. Sastry, "Formation control of nonholonomic mobile robots with omnidirectional visual servoing and motion segmentation," in *Proceedings of the IEEE International Conference on Robotics and Automation (ICRA 03)*, no. 1, (Taipei, Taiwan), pp. 584–589, Sept. 2003.
- [3] N. Cowan, O. Shakerina, R. Vidal, and S. Sastry, "Vision-based follow-the-leader," in *Proceedings of the 2003 IEEE/RSJ International Conference on Intelligent Robots and Systems (IROS 2003)*, no. 2, (Las Vegas, Nevada USA), pp. 1796–1801, Oct. 2003.
- [4] G. Mariottini, G. Pappas, D. Prattichizzo, and K. Daniilidis, "Vision-based localization of leader-follower formations," in *Proceedings of the IEEE Conference on Decision and Control and European Control Conference (CDC-ECC '05)*, (Seville, Spain), pp. 635–640, Dec. 2005.
- [5] N. Moshtagh, A. Jadbabaie, and K. Daniilidis, "Vision-based distributed coordination and flocking of multi-agent systems," in *Proceedings of Robotics: Science and Systems*, (Cambridge, USA), June 2005.
- [6] R. Diestel, *Graph Theory*. New York: Springer-Verlag, 2000.
- [7] H. Tanner, G. Pappas, and V. Kumar, "Leader-to-formation stability," *IEEE Transactions on Robotics and Automation*, vol. 20, pp. 443–455, June 2004.
- [8] H. Khalil, *Nonlinear Systems*. Prentice Hall, Upper Saddle River, NJ, 3rd ed., 2002.
- [9] O. Orqueda, T. Zhang, and R. Fierro, "An output feedback nonlinear decentralized controller design for multiple unmanned vehicle coordination," *submitted to the International Journal on Robust Control*, Oct. 2005.
- [10] A. Atassi and H. Khalil, "A separation principle for the stabilization of a class of nonlinear systems," *IEEE Transactions on Automatic Control*, vol. 44, pp. 1672–1687, Sept. 1999.
- [11] D. Claus and A. Fitzgibbon, "Polyhedral reliable automatic calibration of a marker-based position tracking system," in *Proceedings of the IEEE Workshop on Applications of Computer Vision*, pp. 300–305, Jan. 2005.
- [12] O. Orqueda, J. Figueroa, and O. Agamennoni, "Motion planning and control: From virtual environments to the real world," in *Proceedings of the IFAC International Symposium on Intelligent Components and Instruments for Control Applications (SICICA)*, (Aveiro, Portugal), July 2003.